PRELIMINARY ANALYSIS ON SEISMIC INPUT LOSS AT A PILE FOUNDATION

Kataoka Shojiro[1], Nagaya Kazuhiro[2] and Kaneko Masahiro[3]

Abstract

Seismic input loss may have significant influence on reducing seismic action, especially in short period range, on structures. Strong motion observation systems including accelerometers on free field and a footing were installed after the 2011 event to clarify characteristics of seismic input loss. A preliminary analysis on the seismic input loss observed at a viaduct is introduced.

Introduction

Strong motions with very high intensity in short period were observed during the 2011 East Japan earthquake (e.g. Kuwabara and Yen, 2011) while little damage to bridge structures was found in the vicinity of the strong motion stations. Progress of seismic retrofit, appropriate revision of design specifications, and difference between predominant period of ground motion and natural period of bridge structures can be pointed out. In addition, seismic input loss might have influenced on reducing seismic action, especially in short period range, on the bridge structures. The seismic input loss is a well-known effect in soil-structure interaction caused by self-cancelling of input waves (e.g. Scanlan, 1976) as shown in Figure 1.

Strong motion observation systems including accelerometers on free-field and on footings were installed at three viaducts after the 2011 event to clarify characteristics of seismic input loss. In this paper, strong motion records obtained during small earthquakes at the Sobanokami viaduct, a steel bridge with pile foundations, are presented as well as a preliminary result of FEM analysis using a model that consists of subsurface ground and simple bridge structure with a pile foundation.

The Sobanokami Viaduct and Observed Records

The location and a photo of the Sobanokami viaduct are shown in Figure 2. It is a part of Sanriku Expressway and located in the city of Ishinomaki, Miyagi prefecture. As shown in Figure 3 and Table 1, the viaduct is 514m long and has 9 spans and deep cast-in-situ pile foundations. It was designed under the Design specifications issued in 1996 (JRA, 1996) and completed in 2003. The seismographs were installed at P8 in 2012 as shown in Figure 4. The foundation of P8 has 9 piles with length of 68m.

Figure 5 shows acceleration waveforms and Fourier spectra of the observed

[1] Senior Researcher, Earthquake Disaster Prevention Division, NILIM
[2] Senior Researcher, Earthquake Disaster Prevention Division, NILIM
[3] Head, Earthquake Disaster Prevention Division, NILIM

motion on the free-field and the P8 footing during the off Miyagi earthquake (M4.7) on Feb. 13, 2013. The peak acceleration observed on the free-field is obviously larger than that on the footing. The Fourier spectra on the free-field have rich short period component, while those on the footing do not. Spectral ratios of the ground motions observed on the footing to those on the free-field are shown in Figure 6. The effect of the seismic input loss can be seen; the ratios are about 1 in the period longer than 0.6s but drop to about 0.5 in the period shorter than 0.4s though there are large fluctuations.

In order to carry out a preliminary FEM analysis for earthquake response of subsurface ground with a pile foundation, the ground motion on engineering bedrock at P8 was estimated by a back analysis using SHAKE (Schnabel et al., 1972) with soil properties shown in Table 2 and Figure 7. Acceleration waveforms and response spectra of the observed ground motion at free-field and the estimated engineering bedrock motion are compared in Figure 8. A little nonlinear response effect can be seen in the response spectra in short period.

A Preliminary FEM Analysis for Seismic Input Loss

An analytical model was made for evaluation of seismic input loss at P8 pile foundation of the Sobanokami viaduct as shown in Figure 9. The structure model consists of bearings (linear spring element), RC piers (linear beam element), footing (rigid), and piles (linear beam element). Soil properties are the same as those used in the back analysis to estimate the engineering bedrock motion.

The FEM analysis was carried out using the engineering bedrock motion (Figure 7) as input motion. Figure 10 shows acceleration waveforms and Fourier spectra of the observed and simulated ground motion on the free-field and the footing. The simulated ground motions show a good agreement with the observed ones. Figure 11 compares Fourier spectra of the ground motions on the free-field and the footing. Both of the observed and simulated ones show the same tendency; the ground motions on the free-field have rich short period component while the others does not. Spectral ratios of the ground motions on the footing to those on the free-field are compared in Figure 12. Though the observed one shows much more fluctuation than the simulated result, the effect of seismic input loss can be clearly seen in the both spectral ratios.

Summary

The effect of seismic input loss has been successfully observed by the new strong motion observation system and simulated by the preliminary FEM analysis. It is important to clarify its dependence on types and dimensions of foundations, soil properties, and ground motion characteristics for further improvement of seismic design of bridges and viaducts.

References

Japan Road Association (1996): Design specifications for highway bridges.

Kuwabara, T. and Yen, W. P. (2011): U.S.-Japan Joint Reconnaissance Report of Bridge Damage due to 2011 Tohoku Earthquake, http://www.pwri.go.jp/eng/ujnr/

tohokueq.htm
Scanlan, R. H. (1976): Seismic wave effects on soil-structure interaction, *Earthquake Engineering & Structural Dynamics*, Vol. 4, pp. 379-388.
Schnabel, P. B., Lysmer, J. and Seed, H. B. (1972): SHAKE – A computer program for earthquake response analysis of horizontally layered sites, Report No. EERC 72-12, University of California, Berkeley.

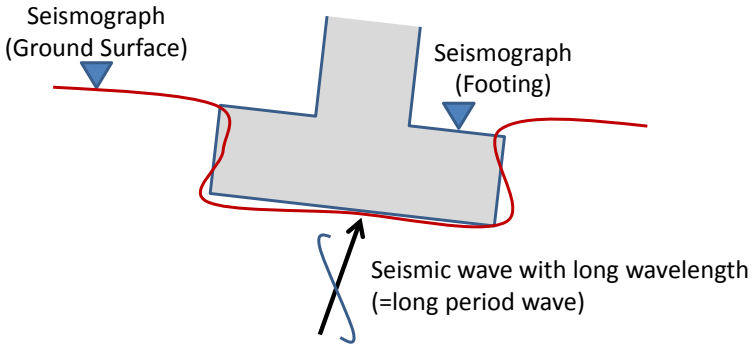

(a) Input motion with long wavelength

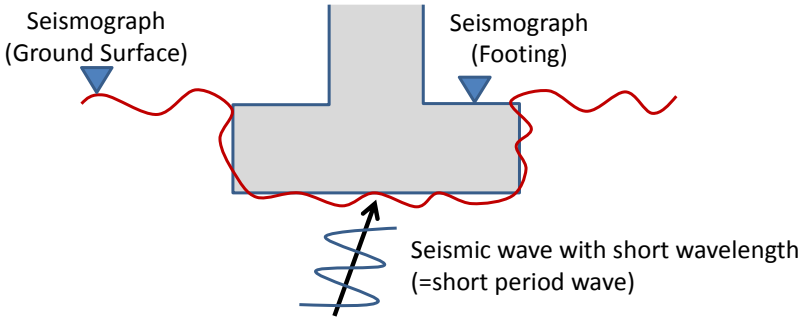

(b) Input motion with short wavelength

Figure 1 Schematic explanation of seismic input loss. A structure footing moves in the same way as ground surface against (a) an input motion with long wavelength but they moves independently against (b) an input motion with short wavelength.

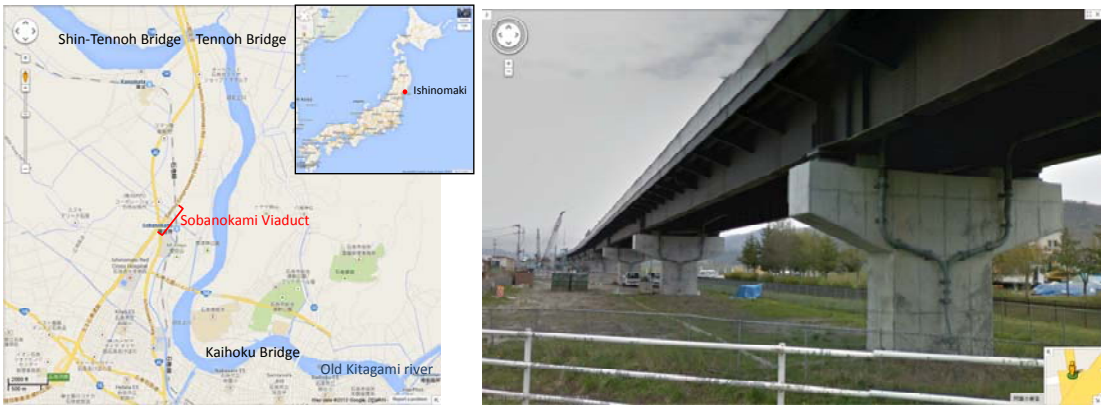

Figure 2 Map showing location of the Sobanokami viaduct and a photo taken from A1 (south) side.

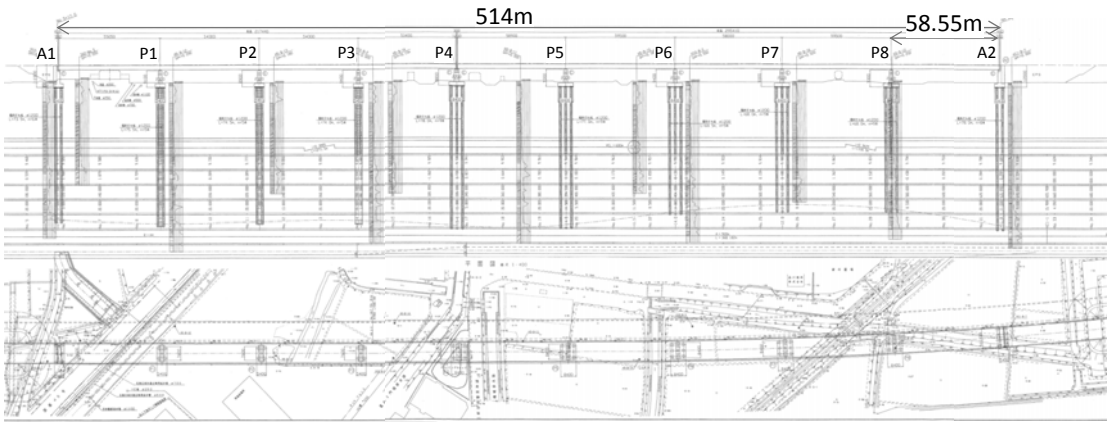

Figure 3 Side and plan views of the Sobanokami viaduct

Table 1 Structural properties

Length/Width	514.0m/11.2m
Span length	55.05+54.0+54.0+53.4m; 58.9+59.5+58.0+59.5+58.55m
Superstructure	4-span & 5-span continuous steel double-I-girders (steel slabs)
Abutment	Inverted T-type, height: 11.9/12.0m (A1/A2)
Pier	T-type RC, height: 7.1/6.9/7.4/6.8/7.3/7.4/7.3/7.3m (P1-8)
Foundation	Cast in-situ pile, ϕ 1.2m; length: 68.0-78.0m; number of piles: 5-9
Bearing	Laminated rubber bearings

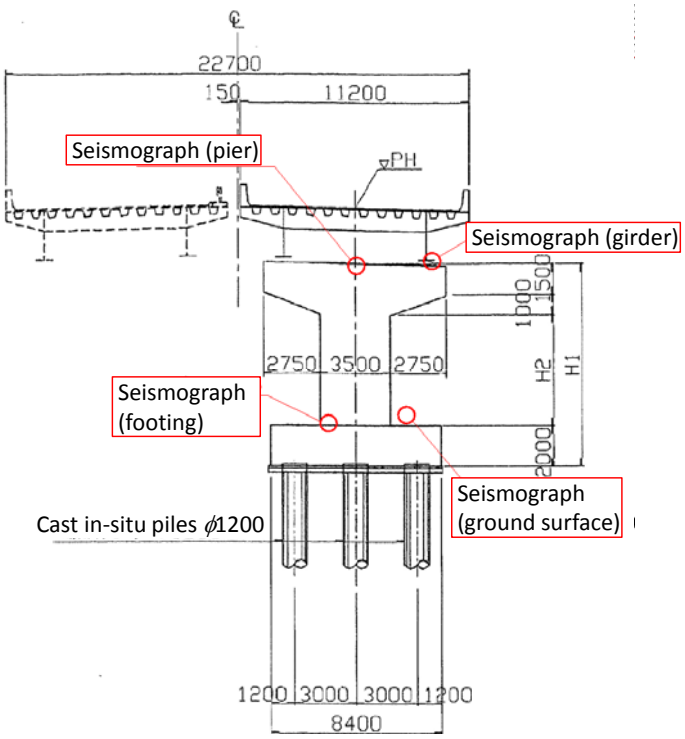

Figure 4 Arrangement of seismographs at P8.

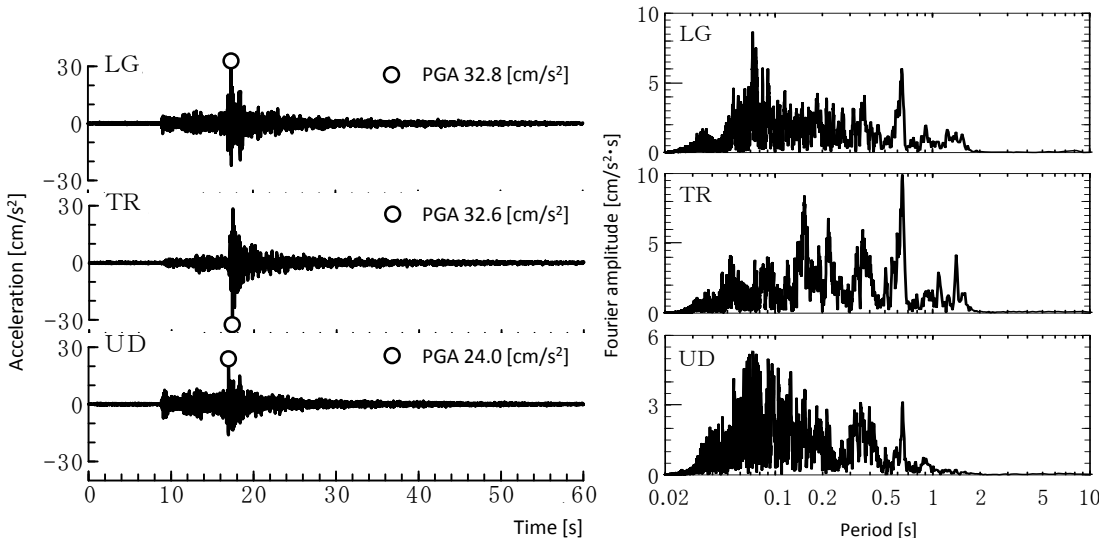

(a) Free-field motion

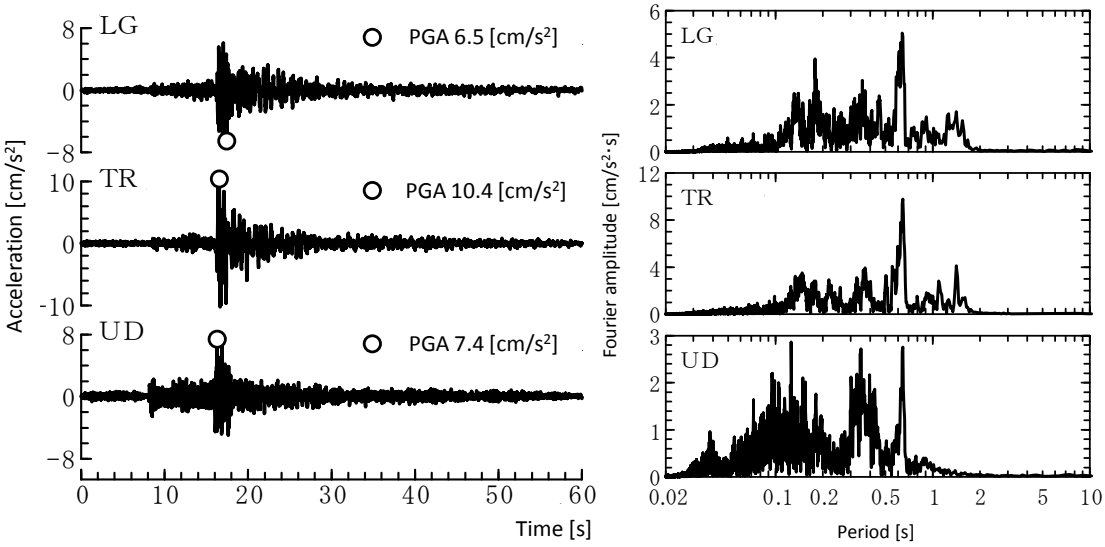

(b) P8 footing

Figure 5 Acceleration waveforms and Fourier spectra of the observed motion on (a) the free-field and (b) the P8 footing during the off Miyagi earthquake (M4.7) on Feb. 13, 2013. LG, TR, and UD denote longitudinal, transverse, and vertical directions, respectively.

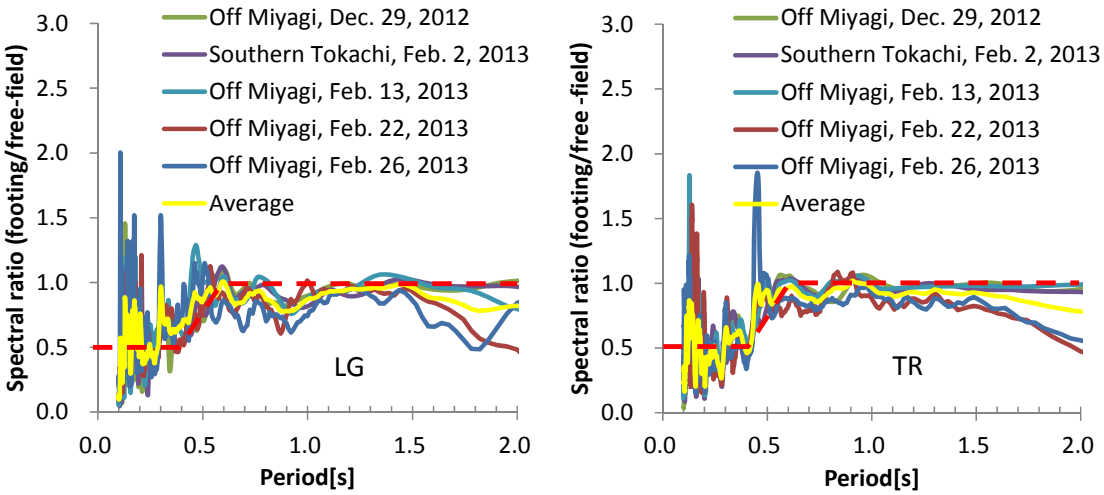

(a) Longitudinal direction (b) Transverse direction

Figure 6 Spectral ratio of the ground motion observed on the footing to that on the free-field during 5 earthquakes. Magnitudes of the earthquakes range from 4.4 to 6.5.

Table 2 Soil properties at P8 of the Sobanokami viaduct. *Vs*, γ, G_D, ν_D, and E_D denote S-wave velocity, unit weight, dynamic shear coefficient, dynamic Poisson's ratio, and dynamic deformation coefficient, respectively.

No.	Depth [m]	Soil classifi-cation	N-value	*Vs* [m/s]	γ [kN/m^3]	G_D [kN/m^2]	ν_D	E_D [kN/m^2]	Key depths
1	-	Clay	1	100	15	1.53E+4	0.45	4.44E+4	Ground water level: 0.08m
2	0.08	Clay	1	100	15	1.53 E+4	0.49	4.56E+4	
3	1.70	Sand	3	115	18	2.45 E+4	0.49	7.29E+4	Underside of footing: 2.62m
4	8.63	Clay	2	126	16	2.59 E+4	0.49	7.72E+4	
5	15.83	Clay	3	144	17	3.61 E+4	0.49	1.08E+5	
6	23.33	Sand	5	137	18	3.44 E+4	0.49	1.02E+5	
7	28.13	Clay	6	182	17	5.73 E+4	0.49	1.71E+5	
8	40.33	Clay	11	222	17	8.58 E+4	0.49	2.56E+5	
9	51.93	Sand	17	206	18	7.77 E+4	0.49	2.32E+5	
10	58.73	Clay	12	229	17	9.09 E+4	0.49	2.71E+5	
11	68.83	Clay	26	296	17	1.52E+5	0.49	4.54E+5	Head of piles: 70.44m
12	78.83	Sand	50<	300<	20	1.84E+5	0.49	5.47E+5	

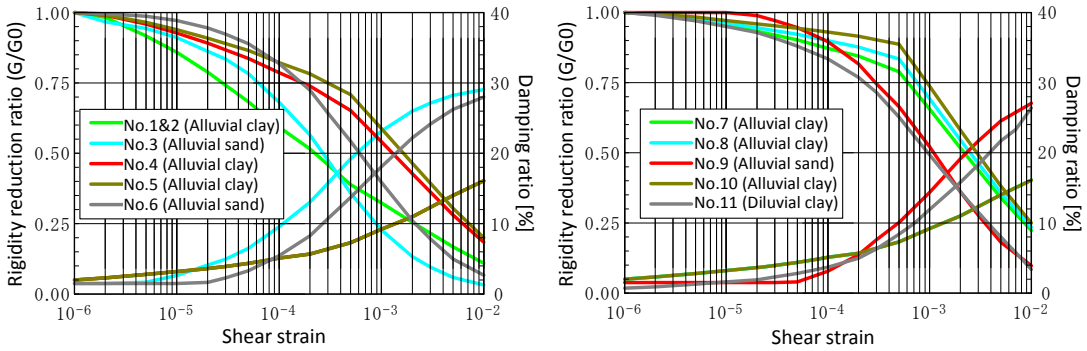

Figure 7 Dynamic properties of the soil layers. The numbers of the layers correspond to those in Table 2.

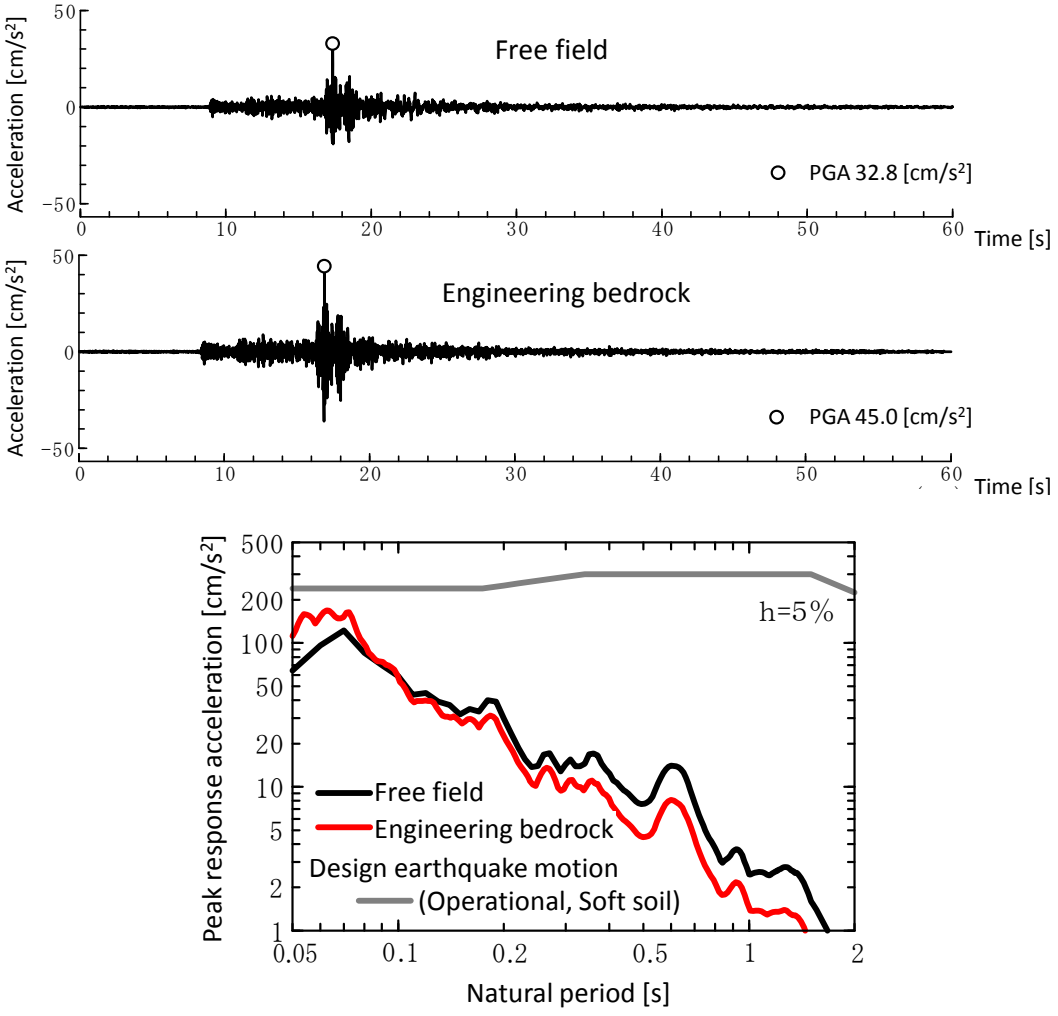

Figure 8 Acceleration waveforms and response spectra of the ground motion in LG direction at free- field and the engineering bedrock.

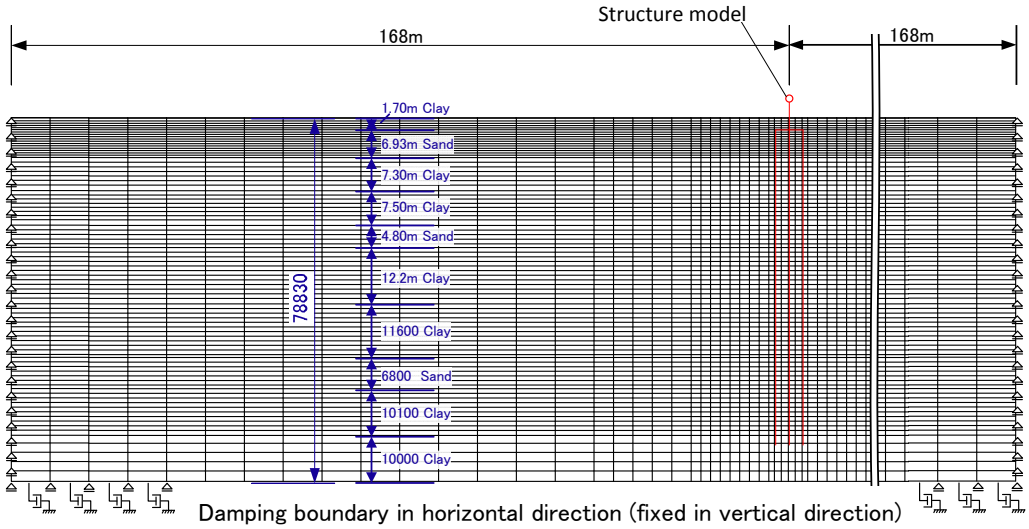

Figure 9 Analytical model for evaluation of seismic input loss at the Sobanokami viaduct. The structure model consists of bearings (linear spring element), RC piers (linear beam element), footing (rigid), and piles (linear beam element). The middle part of right half of the model is omitted.

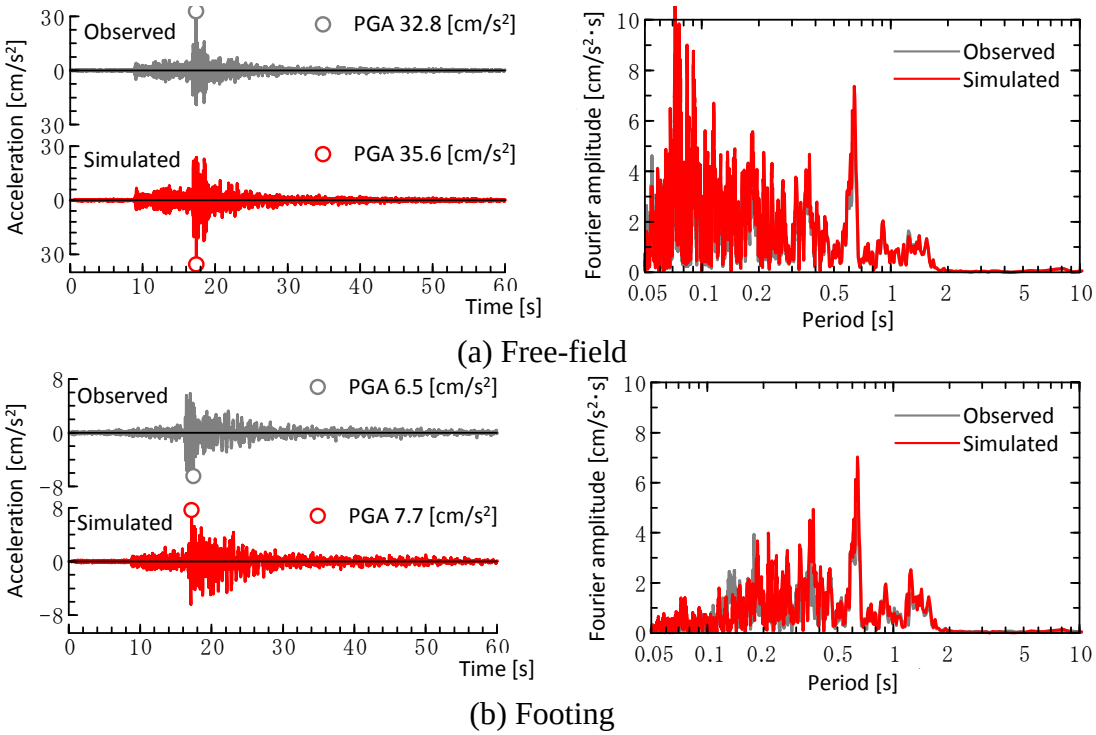

(a) Free-field

(b) Footing

Figure 10 Acceleration waveforms and Fourier spectra of the observed and simulated ground motion on (a) the free-field and (b) the footing.

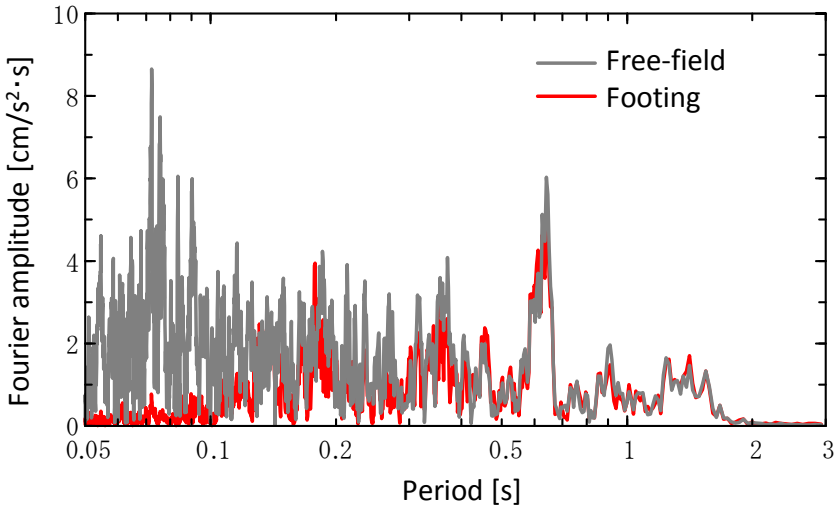

(a) Observed ground motions

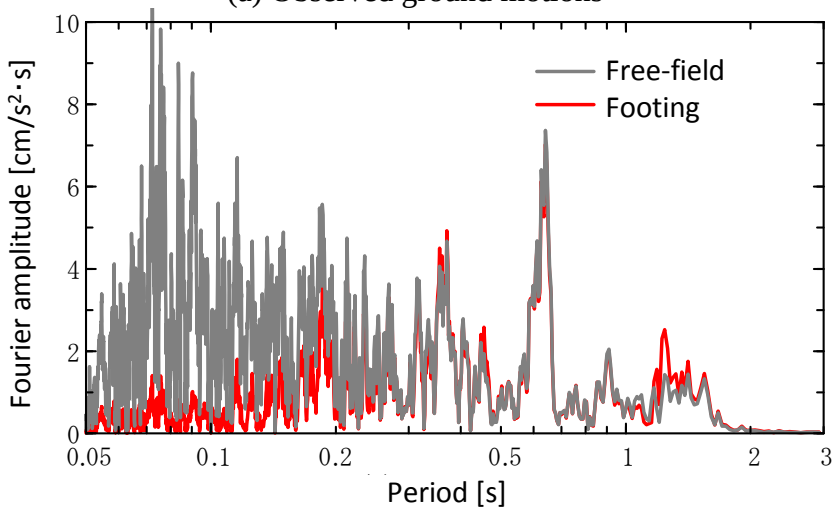

(b) Simulated ground motions

Figure 11 Fourier spectra of the ground motions on the free-field and the footing.

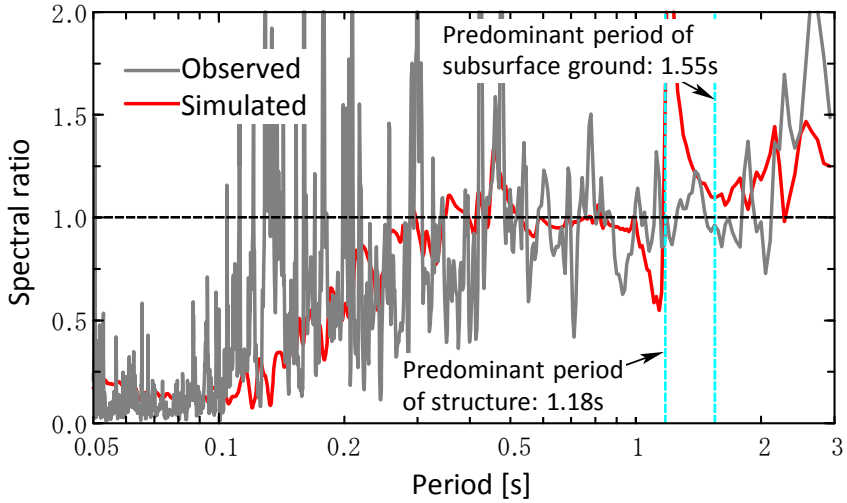

Figure 12 Spectral ratio of the ground motion on the footing to that on the free-field.